

# Gauge Invariance of Resummation Schemes: The QCD Partition Function

M. Achhammer<sup>1</sup>, U. Heinz<sup>2\*</sup>, S. Leupold<sup>1,3</sup>, U. A. Wiedemann<sup>1</sup>

<sup>1</sup>*Institut für Theoretische Physik, Universität Regensburg,*

*D-93040 Regensburg, Germany*

<sup>2</sup>*Cern/TH, CH-1211 Geneva 23*

*Switzerland*

<sup>3</sup>*Institut für Theoretische Physik, Justus-Liebig-Universität Giessen,*

*D-35392 Giessen, Germany*

(December 9, 1996)

We pick up a method originally developed by Cheng and Tsai for vacuum perturbation theory which allows to test the consistency of different sets of Feynman rules on a purely diagrammatic level, making explicit loop calculations superfluous. We generalize it to perturbative calculations in thermal field theory and we show that it can be adapted to check the gauge invariance of physical quantities calculated in improved perturbation schemes. Specifically, we extend this diagrammatic technique to a simple resummation scheme in imaginary time perturbation theory. As an application, we check up to  $\mathcal{O}(g^4)$  in general covariant gauge the gauge invariance of the result for the QCD partition function which was recently obtained in Feynman gauge.

PACS numbers: 12.38.Bx, 11.15.Bt, 11.10.Wx

## I. INTRODUCTION

In finite temperature quantum field theory for massless degrees of freedom, the loop expansion does not coincide with an expansion in orders of the coupling constant. Naive perturbative calculations lead to gauge dependent and infrared divergent results for physical quantities [1]. This necessitates the reorganization of the perturbative expansion in consistent resummation schemes. One of the most important consistency checks for such schemes is the test of their gauge invariance. In practice, this is done mostly by explicit calculations [2], though Ward identities can be used as well [3]. In the vacuum sector, yet another technical tool is at hand. This is a purely diagrammatic method developed by Cheng and Tsai [4] which allows to establish the gauge invariance of a set of Feynman diagrams without carrying out explicit loop calculations. Recently a similar diagrammatic method was independently developed by Feng and Lam [5]. The main motivation of the present work is to undertake a first step in extending the Cheng/Tsai method to resummed perturbative calculations. To this end, we review and slightly extend the approach of Cheng and Tsai presenting a complete set of diagrammatic rules. As an example we show how to check in this approach the gauge invariance of the two loop contribution to the vacuum partition function to  $\mathcal{O}(g^2)$  in general covariant  $\alpha$ -gauge. Then, we extend these rules to a simple resummation scheme.

As a first application, we focus on the gauge invariance up to  $\mathcal{O}(g^4)$  of the QCD partition function. The latter has recently been calculated up to  $\mathcal{O}(g^5)$  [6–8] using a gluon propagator with a resummed static mode. Indeed, there are several reasons for choosing this example. First, the calculations to order  $\mathcal{O}(g^4)$  and  $\mathcal{O}(g^5)$  exist in Feynman gauge only, and the authors did not check the gauge invariance of their results. Since the chosen resummation scheme amounts to the “free” Lagrangian of a massive Yang-Mills field, which is not gauge invariant, invariance of the final result is not automatic. This is different from naive perturbation theory where gauge invariance of observable quantities is automatic if one uses a complete and consistent set of Feynman rules. (For certain gauges this may be a non-trivial problem in itself.) In fact, the method of Cheng and Tsai was invented to study the consistency of different sets of Feynman rules in this respect. Second, in contrast to dynamic quantities of finite temperature QCD which in general require resummed propagators *and* vertices [2], the calculation of the partition function requires only resummed propagators. So, our work extends the method of Cheng and Tsai to the simplest case of a resummation scheme.

In Sec. II we outline the method of Cheng and Tsai [4] and give a short example. In Sec. III we discuss the resummation scheme and some general aspects of the free energy (resp. partition function). As an application we extend the example discussed in Sec. II to finite temperature and prove the gauge invariance of the QCD free energy up to  $\mathcal{O}(g^3)$ . In Sec. IV we discuss a technical issue which arose in the Secs. II and III, the problem of shifting momentum variables. In Sec. V we then prove the gauge invariance of the free energy in finite temperature QCD up to  $\mathcal{O}(g^4)$ .

In the Feynman rules of QCD, the chosen gauge manifests itself in the  $k_\mu$ -dependent part of the free gluon propagator  $D_{\mu\nu}^{ab}$  and in the way  $D_{\mu\nu}^{ab}$  couples to ghosts. We write the gluon propagator in the general form

$$\begin{aligned} D_{\mu\nu}^{ab} &= -i\delta^{ab} [g_{\mu\nu} + a_\mu(-k)k_\nu - a_\nu(k)k_\mu] \frac{1}{k^2 + i\varepsilon} \\ &\equiv D_{F,\mu\nu}^{ab}(k) + \Delta_\mu^{ab}(-k)k_\nu - \Delta_\nu^{ab}(k)k_\mu. \end{aligned} \quad (2.1)$$

Diagrammatically we denote the factor  $k_\mu$  by an arrow-head. The Feynman-propagator  $D_{F,\mu\nu}^{ab}$  is given by

$$D_{F,\mu\nu}^{ab}(k) = -i\delta^{ab} g_{\mu\nu} \frac{1}{k^2 + i\varepsilon} \quad (2.2)$$

and  $\Delta_\mu^{ab}$  is defined as

$$\Delta_\mu^{ab}(k) = -i\delta^{ab} \frac{a_\mu(k)}{k^2 + i\varepsilon}. \quad (2.3)$$

The gauge dependent pieces are contained in the function  $a_\mu(k)$ , e.g.  $a_\mu(k) = \frac{1}{2}(1 - \alpha)\frac{k_\mu}{k^2}$  for covariant  $\alpha$ -gauges. Checking the gauge invariance of a set of Feynman graphs amounts then to the assertion that the result is unaffected by changing  $a_\mu(k)$ , i.e. by choosing a different gauge. In the following we review the method of Cheng and Tsai [4] to do this check diagrammatically.

The free gluon propagator in (2.1) has been separated diagrammatically into its Feynman gauge part  $D_F$  and explicitly gauge dependent parts. In this way the method of Cheng and Tsai allows to disentangle arbitrary diagrams into their Feynman gauge parts and remainder terms. A set of diagrammatic rules is used to test whether the sum of these remainder terms vanishes. If this is the case, the calculation is independent of the particular choice of  $a_\mu(k)$ . The original motivation of Cheng and Tsai was to check by this technique the consistency of the Feynman rules for different gauges [4,9,10]. We shall employ the same technique to show the gauge invariance for quantities calculated in resummation schemes.

### A. The Basic Idea

We start with  $-i\delta^{ab}\frac{a_\mu(k)k_\nu}{k^2+i\varepsilon}$ , the gauge-dependent part of the propagator. We split this term into the two factors  $\Delta_\mu^{ab}(k)$  and  $k_\nu$ . If this is a contribution to an internal line of a Feynman diagram, then  $k_\nu$  is Lorentz-contracted with a vertex. For the case of a 3-gluon-vertex, this contraction results in a very simple structure,

$$k^\nu \Gamma_{\nu\mu\rho}^{abc}(k, q, p) = g f^{abc} [(p^2 g_{\mu\rho} - p_\mu p_\rho) - (q^2 g_{\mu\rho} - q_\mu q_\rho)]. \quad (2.4)$$

Each one of the two terms in square brackets has the structure of a transverse projector  $\mathcal{P}$ , e.g.  $\mathcal{P}_{\mu\rho}(q) = q^2 g_{\mu\rho} - q_\mu q_\rho$ , acting on one of the 2 outgoing lines of the vertex. Note that in what follows we refer to  $\mathcal{P}$  as a “projector” though it does not satisfy the normalization,  $\mathcal{P}^2 \neq \mathcal{P}$ . Diagrammatically, we express (2.4) in the following way:

The blob at the vertex on the l.h.s. indicates that this vertex carries a complete Lorentz structure which has disappeared on the r.h.s. upon contraction. Note that the diagrams on the r.h.s. have opposite sign.  $\mathcal{P}$  acts on the next propagator in the following way:

$$gf^{abc}\mathcal{P}_\mu^\rho(p)D_{\rho\sigma}^{cd}(p) = -igf^{abd}g_{\mu\sigma} - G_\mu^{abd}(p)p_\sigma. \quad (2.6)$$

We represent this equation graphically as

$$\overset{\mathcal{P}}{\text{wavy line}} = - \text{wavy line with arrow} - \overset{G}{\text{wavy line with arrow}}. \quad (2.7)$$

The first term on the r.h.s. of (2.6) is momentum independent; sandwiched between two vertices attached to either end of the line it leads to a contraction of the vertices (cf. (2.17)). It is graphically represented by the so called “contraction arrow”. The  $G$  in the second term on the r.h.s. is nothing but the product of a ghost-gluon vertex and a ghost propagator

$$G_\mu^{abd}(k) = -igf^{abd}[(a \cdot k - 1)k_\mu - k^2 a_\mu] \frac{1}{k^2 + i\epsilon} \quad (2.8)$$

and is therefore called the ghost contribution. For any covariant gauge  $G(k)$  reduces to

$$G_{F,\mu}^{abd}(k) = igf^{abd} \frac{k_\mu}{k^2 + i\epsilon}. \quad (2.9)$$

Putting (2.4) and (2.6), respectively (2.5) and (2.7), together, we have

$$\text{Diagram 1} = - \text{Diagram 2} - \text{Diagram 3} + \text{Diagram 4} + \text{Diagram 5}. \quad (2.10)$$

There are three more diagrammatic rules needed for the decomposition of Feynman diagrams into explicitly gauge dependent and gauge independent parts. The first specifies how  $\mathcal{P}$  acts on  $\Delta$ :

$$gf^{abc}\mathcal{P}_\rho^\mu(q)\Delta_\mu^{cd}(q) = G_\rho^{abd}(q) - G_{F,\rho}^{abd}(q). \quad (2.11)$$

Note that for all covariant gauges  $G_F = G$  and thus the r.h.s. is zero. Therefore we get for covariant gauges using (2.4), (2.6) and (2.11)

$$\text{Diagram 6} = - \text{Diagram 7} - \text{Diagram 8}. \quad (2.12)$$

We will work in general covariant gauge in the following applications, so rule (2.12) will be often used. The second rule concerns the case that an arrow-head  $k_\mu$  acts on a ghost-contribution. It reads

$$\begin{aligned} k^\nu G_\nu^{abc}(q) &= -q^\nu G_\nu^{abc}(q) - p^\nu G_\nu^{abc}(q) \\ &= -igf^{abc} - p^\nu G_\nu^{abc}(q). \end{aligned} \quad (2.13)$$

Graphically we have

$$\text{Diagram with } q, k \text{ incoming, } p \text{ outgoing, vertex } G = - \text{Diagram with } q \text{ incoming, } p \text{ outgoing, vertex } 1 - \text{Diagram with } k \text{ incoming, } p \text{ outgoing, vertex } G, \quad (2.14)$$

where we denote  $igf^{abc}$  by **1**. This relation is a direct consequence of energy-momentum conservation at the vertex. The last rule concerns the case that  $k_\mu$  is connected to a fermion-gluon vertex  $F$ . We have

$$\begin{aligned} S^{mi}(q)k^\mu F_{\mu,ij}^a S^{jn}(p) &= ig\delta^{im}\delta^{jn} \frac{1}{(\not{q} - m_f + i\varepsilon)} k^\mu \gamma_\mu t_{ij}^a \frac{1}{(\not{p} - m_f + i\varepsilon)} \\ &= ig(t^a)^{mn} \left( \frac{1}{\not{q} - m_f + i\varepsilon} - \frac{1}{\not{p} - m_f + i\varepsilon} \right), \end{aligned} \quad (2.15)$$

which will be represented graphically as

$$\text{Diagram with } q, k \text{ incoming, } p \text{ outgoing, vertex } F = - \text{Diagram with } q \text{ incoming, } p \text{ outgoing, vertex } F - \text{Diagram with } k \text{ incoming, } p \text{ outgoing, vertex } F. \quad (2.16)$$

In the last step of eq. (2.15), we have used  $k + q = p$ .

## B. The Basic Identities

In this subsection we give rules which allow to relate gauge dependent parts of diagrams with different topology with each other. This will be used to show that the gauge dependent parts of different diagrams cancel each other. The first rule relates a diagram with a 4-gluon-vertex  $Q$  to those with contraction arrows. It is obtained by applying (2.10) to diagrams with a second three-gluon vertex  $\Gamma$ :

$$\begin{aligned} & ig g^{\nu\phi} f^{abe} \Gamma_{\delta\phi\gamma}^{dec}(-p-k+k', p+k, -k') \\ & - ig g^{\gamma\phi} f^{cae} \Gamma_{\delta\nu\phi}^{dbe}(-p-k+k', k, p-k') \\ & - ig g^{\delta\phi} f^{dae} \Gamma_{\phi\nu\gamma}^{ebc}(k'-k, k, -k') \\ & - p^\mu Q_{\mu\nu\gamma\delta}^{abcd} = 0. \end{aligned} \quad (2.17)$$

The second identity addresses the case that the contraction arrow points at a four-gluon vertex:

$$\begin{aligned} & ig f^{ahg} g^{\mu\phi} Q_{\phi\delta\gamma\nu}^{hdcb} - ig f^{gdh} g^{\delta\phi} Q_{\mu\phi\gamma\nu}^{ahcb} - ig f^{ghc} g^{\gamma\phi} Q_{\mu\delta\phi\nu}^{adhb} + ig f^{bhg} g^{\nu\phi} Q_{\mu\delta\gamma\phi}^{adch} = 0. \end{aligned} \quad (2.18)$$

The third identity (which we have not found in the literature, but which will play an important role in Sec. V) concerns the case that the contraction arrow points at a vertex which carries a  $G$ . This identity follows from the Bianchi identity for the color structure coefficients  $f^{abc}$ :

$$\begin{aligned}
& \text{Diagram 1} - \text{Diagram 2} - \text{Diagram 3} = 0. \\
& igf^{aed}G_{\nu}^{bce}(k) - igf^{bed}G^{\phi,ace}(k)g_{\nu\phi} - igf^{abe}G^{\phi,ecd}(k)g_{\nu\phi} = 0.
\end{aligned} \tag{2.19}$$

The fourth identity treats the case that the contraction arrow points at a fermion-gluon vertex:

$$\begin{aligned}
& \text{Diagram 4} = \text{Diagram 5} - \text{Diagram 6} \\
& -igf^{abe}g^{\nu\phi}F_{\phi,ij}^e(p+k) = \Upsilon_{\nu,ij}^{ab} - \Upsilon_{\nu,ij}^{ba}.
\end{aligned} \tag{2.20}$$

Note that the gluon lines at the four-point fermion-gluon vertex created in (2.16) cannot be interchanged due to the color-structure (cf. Appendix C).

### C. A First Example

To illustrate the method of Cheng and Tsai, we discuss briefly the gauge invariance of the  $\mathcal{O}(g^2)$ , contributions to the QCD partition function. For this purpose we will from now on concentrate on general covariant  $\alpha$ -gauge. That means that we will use the special structure  $G_F = G$ , which the ghost contribution satisfies (cf. 2.11). This leads to the use of eq. (2.12) in the following. The partition function consists of four diagrams <sup>1</sup>:

$$\begin{aligned}
& +\frac{1}{8} \text{(A)} + \frac{1}{12} \text{(B)} - \frac{1}{2} \text{(C)} - \frac{1}{2} \text{(D)}.
\end{aligned} \tag{2.21}$$

The dotted lines are the usual notation for ghost propagators. For our purpose it is however more useful to express diagrams like (2.21.C) in the following way:

$$\text{Diagram (C) rewritten as } G \text{ loop with a wavy line through it.} \tag{2.22}$$

We follow a three step procedure:

We select, one after the other, a diagram in (2.21) and separate the  $a_\mu$ -dependent part of one of the internal gluon lines. E.g. for diagram (2.21.B) this looks like

---

<sup>1</sup>We indexed each diagram with a letter in order to refer to it later in the text (e.g. diagram (2.21.C) is the third diagram in (2.21)). Moreover we give the factor (-1) for the fermion and ghost loops in the following explicitly in the symmetry factor.

$$\begin{array}{c} \text{(A)} \end{array} D = \begin{array}{c} \text{(B)} \end{array} D_F + \Delta \begin{array}{c} \text{(C)} \end{array} - \begin{array}{c} \text{(D)} \end{array} \Delta . \quad (2.23)$$

Because  $\Delta$  is proportional to an odd power of the momentum  $k$  diagrams (2.23.C) and (2.23.D) can be summed. So we get:

$$\begin{array}{c} \text{(A)} \end{array} D = \begin{array}{c} \text{(B)} \end{array} D_F + 2 \Delta \begin{array}{c} \text{(C)} \end{array} . \quad (2.24)$$

Next we use the rules of Sec. IIA to decompose diagram (2.24.C):

$$\begin{aligned}
& \Delta \begin{array}{c} \text{(A)} \end{array} \stackrel{(2.10)}{=} + \Delta \begin{array}{c} \text{Diagram 1} \end{array} + \Delta \begin{array}{c} \text{Diagram 2} \end{array} - \Delta \begin{array}{c} \text{Diagram 3} \end{array} - \Delta \begin{array}{c} \text{Diagram 4} \end{array} \\
& \quad = +2 \left[ \Delta \begin{array}{c} \text{Diagram 1} \end{array} - \Delta \begin{array}{c} \text{Diagram 5} \end{array} \right] \\
& \stackrel{(2.10)}{=} \stackrel{(2.12)}{=} + 2 \left[ \Delta \begin{array}{c} \text{Diagram 1} \end{array} - \Delta \begin{array}{c} \text{Diagram 6} \end{array} - \begin{array}{c} G \end{array} \begin{array}{c} \text{Diagram 7} \end{array} \right] \\
& \stackrel{(2.14)}{=} + 2 \left[ \Delta \begin{array}{c} \text{(B)} \end{array} - \Delta \begin{array}{c} \text{(C)} \end{array} + \begin{array}{c} G \end{array} \begin{array}{c} \text{(D)} \end{array} + \begin{array}{c} G \end{array} \begin{array}{c} \text{(E)} \end{array} \right] . \quad (2.25)
\end{aligned}$$

As a second step, we invoke the identities of Sec. IIB as follows. Connecting the external lines of eq. (2.17), we get

$$(A) - (B) - (C) - (D) = 0. \quad (2.26)$$

First we observe that diagram (2.26.C) is zero due to the color structure. Obviously diagram (2.26.A) and (2.26.B) look very similar, and after substituting  $-k$  to  $k$  in diagram (2.26.B) we arrive at

$$(A) - (B) = -2 \times (\text{circular loop with } k \text{ and } p). \quad (2.27)$$

Clearly momentum shifts do not affect the value of a complete Feynman diagram. Here, however the integrand of a complete Feynman diagram is rewritten algebraically as a sum and the sequence of the summation and the integration over the internal momentum loop variables is interchanged. Performing the same change of integration variables in all terms of the sum does not effect the result. However, changing integration variables only in some terms, as e.g. in eq. (2.27), requires a careful study of the corresponding terms in the sum. Here, this amounts to the demand that  $a_\mu(k)$  is not too singular to allow for this substitutions and shifts (c.f. [4]). In section IV, we shall show that this subtlety does not obstruct the arguments made in what follows. Altogether we get from (2.26) using (2.27) and attaching a  $\Delta$

$$(A) = -\frac{1}{2} (B). \quad (2.28)$$

Similarly, eq. (2.19) leads to the identity

$$(A) = (B). \quad (2.29)$$

This means that (2.25.C) cancels (2.25.D). Using (2.28), eq. (2.25) is thus simplified to

$$(A) = - (B) + 2 (C). \quad (2.30)$$

Obviously this relates the three different diagrams (2.21.A), (2.21.B) and (2.21.C).

We are now still left with the diagram (2.21.D). Using (2.15) we can make the following decomposition (2.16):

$$(A) = (B) - (C) \quad (2.31)$$

Closing identity (2.20) on the right and left side to loops and attaching a  $\Delta$  one can see that the r.h.s. of eq. (2.31) is zero and in this way the  $a_\mu$ -dependent part of (2.21.D) vanishes.

In the third and final step, one just has to count symmetry factors in order to show that all  $a_\mu$ -dependent terms in (2.21) cancel each other. To do so we count the different ways to obtain the diagrams in (2.30) from (2.21). There are 6 possibilities to assign  $\Delta_\mu k_\nu$  to diagram (2.21.B): there are 3 lines to choose from and 2 ends of the line to which the factor  $\Delta$  can be attached. (The latter factor 2 is explicitly given in (2.24).) Similarly, there are 4 such possibilities for diagram (2.21.A) and 2 for (2.21.C). This counting shows immediately that all terms linear in  $\Delta_\mu k_\nu$  cancel each other. Similarly one can show the same for the terms which are quadratic and cubic in  $\Delta_\mu k_\nu$ . That is all we have to show: (2.21) leads to the same result whether we calculate it in an arbitrary  $\alpha$ -gauge or in the Feynman gauge.

#### D. The Symmetrization Argument

Arguing separately for each order of  $\Delta_\mu k_\nu$  is very hard to do for more complicated diagram. In this subsection we outline a technique for solving this problem which is based on the following observation: In principle gauge invariance of a sum of diagrams requires only that this sum does not change if  $a_\mu$  is simultaneously changed in *all* lines of the diagrams. However, we will show in the following that the same sum of diagrams remains unchanged even if  $a_\mu$  is changed in only *one* line in *each* diagram. To see this we start again with the sum given in (2.21) and symmetrize the diagrams with respect to the gluon propagators:

$$\begin{aligned} & \frac{1}{12} \left[ \begin{array}{c} \text{Diagram (A): Circle with wavy line } D_2 \text{ and vertices } D_1, D_3 \\ \text{Diagram (B): Two circles, top } D_1, \text{ bottom } D_2 \\ \text{Diagram (C): Two circles, top } D_1, \text{ bottom } D_3 \\ \text{Diagram (D): Two circles, top } D_2, \text{ bottom } D_3 \end{array} \right] \\ & - 2 \left[ \begin{array}{c} \text{Diagram (E): Circle with wavy line } D_1 \text{ and vertices } G, G \\ \text{Diagram (F): Circle with wavy line } D_2 \text{ and vertices } G, G \\ \text{Diagram (G): Circle with wavy line } D_3 \text{ and vertices } G, G \end{array} \right] \end{aligned}$$

$$-2 \left( \begin{array}{c} \text{Diagram (H)} \\ \text{Diagram (I)} \\ \text{Diagram (J)} \end{array} \right). \quad (2.32)$$

In the spirit of Sec. IIC, we choose now one line, say  $D_1$ , and split it into its gauge dependent and independent parts. This means e.g. for (2.32.A):

$$\begin{array}{c} D_1 \\ \text{Diagram (A)} \end{array} = \begin{array}{c} D_{1,F} \\ \text{Diagram (B)} \end{array} + 2 \Delta \begin{array}{c} \text{Diagram (C)} \end{array} \quad (2.33)$$

Clearly all diagrams in (2.32) containing  $D_1$  must be treated in the same way. According to (2.31) the fermion diagram cancels immediately. By complete analogy with our treatment in eq. (2.25), one observes that the gauge-dependent part arising from the propagator  $D_1$  in (2.33) cancels the corresponding gauge-dependent contributions of  $D_1$  in (2.32.B/C/E). Consequently, we can replace in (2.32) the propagator  $D_1$  by its Feynman part  $D_{1,F}$  without changing  $D_2$  and  $D_3$ . In the procedure the explicit form of  $D_2$  and  $D_3$  is never used. As we have changed  $D_1$  to  $D_{1,F}$  without changing the value of the whole sum of diagrams we can do the same for  $D_2$  and finally also for  $D_3$ . Consequently,  $D_2$  and  $D_3$  can also be replaced by their Feynman parts  $D_{2,F}$  and  $D_{3,F}$  without changing the value of (2.32). The set of diagrams has the same value in Feynman gauge and in all  $\alpha$ -gauges and in this sense it is gauge-invariant.

From the fact that  $D_1$  can be replaced by  $D_{1,F}$  without using the explicit form of  $D_2$  and  $D_3$ , we draw two conclusions:

1. It is sufficient to check the invariance of a set of Feynman diagrams under the replacement of only one propagator in each diagram by its Feynman part. The rest can be handled by symmetrization.
2. Since no assumption is made about the form of the  $D_n$ , each could enter the symmetrized expression with a different  $\Delta_\mu k_\nu$  without affecting the result of the calculation.

In the next section we will generalize the diagrammatic rules presented here to the case of finite temperature.

### III. THE CHENG-TSAI METHOD FOR IMAGINARY TIME PERTURBATION THEORY

So far, we have reviewed and completed the basic Cheng-Tsai rules for vacuum QCD. Now we explain in a first step how these rules get modified in imaginary time perturbation theory at finite temperature (i.e. with a compact imaginary time coordinate). Subsequently, the rules are extended to a resummed perturbation scheme in which a dynamically generated Debye screening mass is introduced for the static temporal gauge propagator. This paves the way for checking the gauge invariance of the  $\mathcal{O}(g^4)$  result for  $Z_{\text{QCD}}$ .

#### A. Diagrammatic Cheng-Tsai Rules at Finite Temperature

The Feynman rules for imaginary time perturbation theory at finite temperature differ from the vacuum ones essentially only by changing the energy component  $k_0$  of the four momentum  $k$  to discrete imaginary Matsubara frequencies,  $k_0 = i2n\pi\beta^{-1}$  for bosons,  $k_0 = i(2n+1)\pi\beta^{-1}$  for fermions with  $\beta$  being the inverse temperature. This leads to the replacement of loop integrals in momentum space by

$$\int \frac{d^4 k}{(2\pi)^4 i} \rightarrow \beta \sum_{k_0} \int \frac{d^3 k}{(2\pi)^3}. \quad (3.1)$$

The energy-momentum conservation at each vertex is modified accordingly:

$$i(2\pi)^4 \delta(k) \rightarrow \beta(2\pi)^3 \delta_{n0} \delta(\vec{k}). \quad (3.2)$$

Up to factors  $i$  coming from the imaginary  $k_0$  components, the propagators and vertices look formally the same as in the vacuum case, now being functions of  $\vec{k}$  and  $k_0$  (cf. Appendix B). They can be split up diagrammatically into their Feynman gauge and explicit  $a_\mu$ -dependent parts in exactly the same way as before, e.g.

$$\begin{aligned} D_{\mu\nu}^{ab} &= \delta^{ab} [g_{\mu\nu} + a_\mu(-k)k_\nu - a_\nu(k)k_\mu] \frac{1}{k^2}, \\ &\equiv D_{F,\mu\nu} + \Delta_\mu(-k)k_\nu - \Delta_\nu(k)k_\mu; \quad \text{with } k^2 = \vec{k}^2 + k_0^2, \end{aligned} \quad (3.3)$$

$$\text{~~~~~} = \text{~~~~~}^{D_F} + \text{~~~~~}^{\Delta} \rightarrow - \text{~~~~~}^{\Delta} \text{~~~~~},$$

where now the Feynman propagator is defined by

$$D_{F,\mu\nu}^{ab} = \delta^{ab} g_{\mu\nu} \frac{1}{k^2} \quad (3.4)$$

while  $\Delta_\mu^{ab}$  takes the form

$$\Delta_\mu^{ab}(k) = \delta^{ab} \frac{a_\mu(k)}{k^2}. \quad (3.5)$$

With these changes, the diagrammatic rules (2.10), (2.12), (2.14) and (2.16) look the same, the ghost contribution reading now (c.f. (2.8))

$$G_\mu^{abd}(k) = -i f^{abd} [(a \cdot k - 1) k_\mu - k^2 a_\mu] \frac{1}{k^2}. \quad (3.6)$$

Also, the basic identities (2.17-2.20) carry over without further modification. Note that the application of the Cheng-Tsai method in imaginary time perturbation theory proceeds as in the vacuum case. It is not obstructed by the replacement (3.1). All rules are purely algebraic, establishing the cancellation of  $a_\mu$ -dependent terms on the level of the integrand before any loop integrations are performed (for a detailed discussion, cf. Sec. IV). Consequently, they do not depend on changing the  $k_0$ -loop integral to an infinite sum.

## B. A Simple Resummation Scheme

As already mentioned, naive calculations in finite temperature perturbation theory with massless degrees of freedom can lead to gauge dependent and infrared divergent results for physical quantities since the loop expansion does not coincide with an expansion in orders of the coupling constant [1]. Depending on the physical quantity one wants to calculate, this requires the use of more or less refined resummation schemes [2,11,12]. A prominent example is the QCD partition function  $Z_{\text{QCD}}$  for which naive perturbation theory leads to an incomplete two-loop result, missing the  $\mathcal{O}(g^3)$ -contribution completely, and becomes infrared divergent at the three-loop level. At least up to order  $\mathcal{O}(g^5)$ , a consistent resummation scheme curing all infrared divergences is obtained by reorganizing perturbation theory with a massive static  $A_0$ -propagator [7,11].

$$\mathcal{L} = \left( \mathcal{L} + \frac{1}{2} m^2 A_0^a A_0^a \delta_{k_0,0} \right) - \frac{1}{2} m^2 A_0^a A_0^a \delta_{k_0,0}. \quad (3.7)$$

Here,  $m$  denotes the dynamical generated Debye screening mass which takes into account the screening of electric fields in a polarizable plasma at finite temperature and density. At lowest order in the coupling constant the Debye mass is obtained as the infrared limit of the corresponding component of the one-loop self energy  $\Pi_{\mu\nu}$ ,

$$m^2 = \lim_{\vec{k} \rightarrow 0} \Pi_{00}(k_0 = 0, \vec{k}). \quad (3.8)$$

$$-\Pi_{\mu\nu} = \frac{1}{2} \text{ (self-energy diagram)} + \frac{1}{2} \text{ (polarization bubble)} - \text{ (ghost loop)} - \text{ (triangle diagram)} \quad (3.9)$$

In the improved imaginary time perturbation theory, resummed according to (3.7) and (3.9), the gauge boson propagator reads

$$\begin{aligned} D_{\mu\nu}^{ab}(k) &= \delta^{ab} \left[ g_{\mu\nu} + a_\mu(-k)k_\nu - a_\nu(k)k_\mu - \delta_{\mu 0}\delta_{\nu 0}\delta_{k_0 0} \frac{m^2}{m^2 + k^2} \right] \frac{1}{k^2}, \\ &\equiv \underbrace{D_{F,\mu\nu}^{ab} - \delta^{ab}\delta_{\mu 0}\delta_{\nu 0}\delta_{k_0 0} \frac{m^2}{k^2(m^2 + k^2)}}_{D_{F,\mu\nu}^{'ab}} + \Delta_\mu(-k)k_\nu - \Delta_\nu(k)k_\mu. \end{aligned} \quad (3.10)$$

$$\text{wavy line} = \text{wavy line with } D_F' \text{ label} + \text{wavy line with } \Delta \text{ label and arrow} - \text{wavy line with } \Delta \text{ label and arrow} \quad (3.11)$$

The counterterm in (3.7) is treated diagrammatically as a new two-point vertex

$$\text{a} \text{---} \text{wavy line} \text{---} \text{b} = \delta^{ab}\delta_{\nu 0}\delta_{\mu 0}\delta_{k_0 0}m^2 \quad (3.12)$$

Note that the counter term in (3.7) breaks the gauge invariance explicitly. Hence, it is a priori unclear whether this reorganization of perturbation theory preserves the gauge invariance at a fixed order in the coupling constant. Due to the mass term in (3.10), the Cheng-Tsai rule for the action of the “projection”  $\mathcal{P}$  on the propagator  $D_{\mu\nu}^{ab}$  receives now an extra contribution

$$-igf^{abc}\mathcal{P}_\mu^\rho D_{\rho\nu}^{cd}(k) = igf^{abd}\delta_{\mu 0}\delta_{\nu 0}\delta_{k_0 0} \frac{m^2}{m^2 + k^2} - igf^{abd}g_{\mu\nu} - G_\mu^{abd}(k)k_\nu. \quad (3.13)$$

$$\mathcal{P} \text{ wavy line} = + \text{wavy line with } \times \text{ and } + \text{ label} - \text{wavy line with } \rightarrow \text{ label} - \text{wavy line with } G \text{ label and arrow}$$

Thus (2.10) is modified to

$$\text{Diagram} = + \text{Diagram} - \text{Diagram} - \text{Diagram} - \text{Diagram} + \text{Diagram} + \text{Diagram} \quad (3.14)$$

Since eq. (3.7) does not involve resummed vertices, all Cheng-Tsai rules relating different vertices to each other remain unchanged. Consequently, we have the diagrammatic reformulation of the energy-momentum conservation (2.14), the fermion-vertex rule (2.16) and the basic identities (2.17-2.20) at our disposal. Additionally, there is a rule linking the counter term (3.12) to the mass-dependent term in (3.13):

$$igf^{abe}g_{\mu\sigma}\delta_{\sigma 0}\delta_{\alpha 0}\delta_{k_0 0}m^2D^{ed,\alpha}{}_{\nu}(k) = igf^{abd}\delta_{\mu 0}\delta_{\nu 0}\delta_{k_0 0}\frac{m^2}{m^2+k^2} \quad (3.15)$$

$$\text{Diagram} = \text{Diagram}$$

### C. The QCD Partition Function

With the improved imaginary time perturbation scheme described in the last subsection, the QCD partition function has been calculated to  $\mathcal{O}(g^5)$  [6–8]. Since it is our main aim to check the gauge invariance of these results, let us shortly recall them.

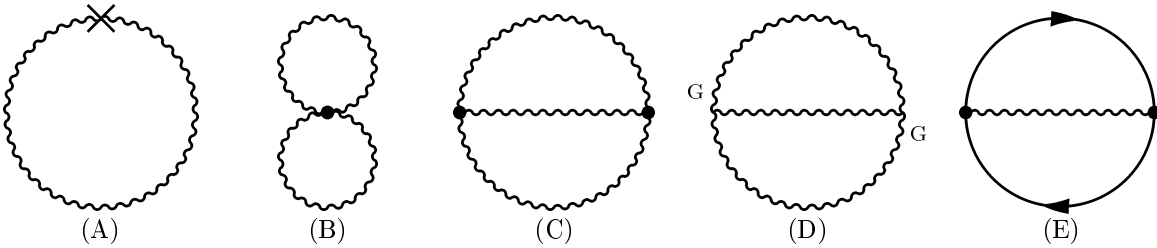
$Z_{\text{QCD}}$  is given by the trace

$$Z_{\text{QCD}} = \text{Tre}^{-\beta H} \quad (3.16)$$

where the Hamiltonian is defined in terms of (3.7). The corresponding free energy is

$$F = -\frac{T}{V} \ln Z_{\text{QCD}}. \quad (3.17)$$

Its lowest order contribution is the Stefan-Boltzmann part, which is diagrammatically represented through one loop diagrams and has been calculated in many different gauges (c.f. [13]). The higher order corrections to this free part can be represented diagrammatically up to  $\mathcal{O}(g^5)$  as follows:



(F) (G) (H) (I) (J)

(K) (L) (M) (N) (O)

(3.18)

Here, the Feynman rules of section III B are understood, and the blob is defined in terms of the self-energy of (3.9) as

$$\text{wavy line with blob} = -\Pi_{\mu\nu} + \text{wavy line with cross} \quad (3.19)$$

The complete  $\mathcal{O}(g^3)$  result of these contributions has been obtained by Kapusta [14] nearly two decades ago. It is given via the resummed two-loop calculation including the diagrams (3.18.A-E), and was obtained in [14] in Feynman gauge. Only recently, Arnold and Zhai have calculated the  $\mathcal{O}(g^4)$  contributions [6,7], being able to reduce all occurring loop integrals to standard ones and to the so-called scalar basketball diagram. At this order all mass terms can be neglected in the 3-loop diagrams. With essentially the same methods but including the mass terms in the three-loop diagrams, the calculation was pushed to  $\mathcal{O}(g^5)$  by Zhai and Kastening [8]. Beyond  $\mathcal{O}(g^5)$ , simple resummation based on (3.7) is known to lead to infrared divergences. This is the Linde argument [15,16] that diagrams with arbitrarily high numbers of loops all contribute to  $\mathcal{O}(g^6)$ . However it is possible to organize the 6th order contribution into the two terms  $c_1 g^6$  and  $c_2 g^6 \ln g$  as it is done in lattice calculations [17]; then other resummation techniques [12] may give access to  $c_2$ , while  $c_1$  must be computed numerically. For a more extensive review of the resummation techniques in order to calculate quantities as e.g.  $Z_{\text{QCD}}$ , we refer to [18].

#### D. From Two Loop Vacuum Diagrams to Free Energy at $\mathcal{O}(g^3)$

The gauge invariance of diagrams (3.18.B-E) for the vacuum case has already been discussed in Sec. II. Since the decomposition rule (2.6) has changed to (3.13), additional diagrams appear, namely

(3.20)

Both diagrams are of  $\mathcal{O}(g^4)$  and, as we will see in section V, cancel diagrams stemming from  $\mathcal{O}(g^4)$  counter terms. Clearly these diagrams should be neglected in a calculation which is only accurate to  $\mathcal{O}(g^3)$ . Hence the obtained result for  $Z_{\text{QCD}}$  up to  $\mathcal{O}(g^3)$  is  $\alpha$ -independent.

In the previous Sections we have shown how powerful the diagrammatic method of Cheng and Tsai is. However, we have not discussed one crucial technicality, which is the subject of the present Section. Namely if various diagrams are related to each other (like in (2.27)), shifts in the momenta have to be performed before the diagrams are really algebraically identical. This requires that the used propagators are not too singular. Otherwise shifting momenta might change the result of a loop integral and thus diagrams like (2.28.A) and (2.28.B) would *not* cancel each other. Therefore naively using the Cheng-Tsai method and ignoring this problem can lead to serious inconsistencies. Indeed, one of the major results of the original Cheng/Tsai work was to point out the subtlety that the widely used naive versions of the different sets of temporal and Coulomb gauge Feynman rules are inconsistent with basic principles. This can be traced back to inappropriate shifts of loop momenta [4,9].

First we recall that momentum shifts are necessary to connect the gauge dependent parts of different diagrams (c.f. (2.27), (2.28)). As long as the involved propagators have no singularities shifting momenta in loop integrals causes no trouble. This might change if the propagators have poles. To see this we study the temporal gauge with its gauge condition

$$A_0 = 0. \quad (4.1)$$

Naively one expects the ghost fields to decouple and the gluon propagator to be

$$D^{ij}(k) = -\frac{i}{k^2 + i\varepsilon} \left( g^{ij} + \frac{k^i k^j}{\vec{k}^2} \right) + \frac{i}{k_0^2} \frac{k^i k^j}{\vec{k}^2} \quad (4.2)$$

$$D^{\mu 0}(k) = D^{0\mu}(k) = 0 \quad (4.3)$$

This is of course a special case of the general form (2.1) with the choice

$$a_\mu(k) = +\frac{g_{\mu 0}}{k_0} - \frac{k_\mu}{2k_0^2}. \quad (4.4)$$

However the spatially longitudinal part of the free temporal propagator has a double pole at  $k_0 = 0$  making momentum shifts difficult to control. To perform loop calculations one must introduce a pole prescription which obviously changes  $a_\mu$ . We choose

$$a_\mu(k) = +g_{\mu 0} \frac{1}{2} \left[ \frac{1}{k_0 + i\eta} + \frac{1}{k_0 - i\eta} \right] - k_\mu \frac{1}{4} \left[ \frac{1}{(k_0 + i\eta)^2} + \frac{1}{(k_0 - i\eta)^2} \right]. \quad (4.5)$$

Thus the longitudinal part of the gauge propagator becomes

$$\begin{aligned} D_L(k) &:= \frac{k_i k_j}{\vec{k}^2} D_{ij}(k) \\ &= \frac{i}{2} \left[ \frac{1}{(k_0 + i\eta)^2} \left( 1 + \frac{2ik_0\eta - \eta^2}{k^2 + i\epsilon} \right) + \frac{1}{(k_0 - i\eta)^2} \left( 1 + \frac{-2ik_0\eta - \eta^2}{k^2 + i\epsilon} \right) \right] \\ &= \frac{i}{2} \left[ \frac{1}{(k_0 + i\eta)^2} + \frac{1}{(k_0 - i\eta)^2} \right] + \mathcal{O}(\eta). \end{aligned} \quad (4.6)$$

Note that this yields the principal value prescription of the  $k_0$ -pole, which was frequently used for loop calculations in temporal gauge until it turned out that the results disagree with Feynman gauge calculation [19]. It reintroduces the ghost field

$$G_\mu^{abc} = +igf^{abc} \frac{\eta^2 k_\mu + g_{\mu 0} k^2 k_0}{(k^2 + i\epsilon)(k_0^2 + \eta^2)} \quad (4.7)$$

and the temporal mode

$$D_{00} = -\frac{i}{k^2 + i\epsilon} \left[ -\frac{\eta^2}{2(k_0 + i\eta)^2} - \frac{\eta^2}{2(k_0 - i\eta)^2} \right]. \quad (4.8)$$

Note that the expressions (4.6), (4.7) and (4.8) are easily calculated by inserting (4.5) in (2.1) and (2.8).

Naively one expects that all the contributions involving ghosts and/or temporal gauge modes vanish for  $\eta \rightarrow 0$  due to the appearance of  $\eta^2$  in the numerators of (4.7) and (4.8). But this is not true as we will show now. Let us concentrate on a two-loop vacuum diagram with two longitudinal (L) and one temporal (O) propagator, as shown in fig. 4.9 [9].

If  $\eta$  is taken to zero *before* the loop integrations are performed there would be no contribution from this diagram since the temporal part (4.8) of the gluon propagator vanishes in this limit. But  $\eta$  serves as a regulator for the  $k_0$ -pole in (4.6) and should be taken to zero only *after* the energy integrations are performed. To check whether there is a contribution in this limit we restrict ourselves to the leading term in  $\eta$ , i.e. we take into account only the first contribution of (4.6). Thus we have to calculate (c.f. 4.9)

$$\begin{aligned} & \int dk_0 dp_0 (k-p)_0 g^{ii'} (k-p)_0 g^{jj'} \frac{k_i k_j}{\vec{k}^2} D_L(k) \frac{p_{i'} p_{j'}}{p^2} D_L(p) D_{00}(k+p) \\ & \sim \int dk_0 dp_0 (k_0 - p_0)^2 \left[ \frac{1}{(k_0 + i\eta)^2} + \frac{1}{(k_0 - i\eta)^2} \right] \left[ \frac{1}{(p_0 + i\eta)^2} + \frac{1}{(p_0 - i\eta)^2} \right] \\ & \quad \times \frac{1}{(k+p)^2 + i\epsilon} \left[ \frac{\eta^2}{(k_0 + p_0 + i\eta)^2} + \frac{\eta^2}{(k_0 + p_0 - i\eta)^2} \right]. \end{aligned} \quad (4.10)$$

By scaling  $k_0 = \kappa_0 \eta$ ,  $p_0 = \pi_0 \eta$  we get

$$\begin{aligned} & \int d\kappa_0 d\pi_0 (\kappa_0 - \pi_0)^2 \left[ \frac{1}{(\kappa_0 + i)^2} + \frac{1}{(\kappa_0 - i)^2} \right] \left[ \frac{1}{(\pi_0 + i)^2} + \frac{1}{(\pi_0 - i)^2} \right] \\ & \quad \times \frac{1}{\eta^2 (\kappa + \pi)^2 - (\vec{k} + \vec{p})^2 + i\epsilon} \left[ \frac{1}{(\kappa_0 + \pi_0 + i)^2} + \frac{1}{(\kappa_0 + \pi_0 - i)^2} \right] \\ & \xrightarrow{\eta \rightarrow 0} \frac{-1}{(\vec{k} + \vec{p})^2} \int d\kappa_0 d\pi_0 (\kappa_0 - \pi_0)^2 \left[ \frac{1}{(\kappa_0 + i)^2} + \frac{1}{(\kappa_0 - i)^2} \right] \left[ \frac{1}{(\pi_0 + i)^2} + \frac{1}{(\pi_0 - i)^2} \right] \\ & \quad \times \left[ \frac{1}{(\kappa_0 + \pi_0 + i)^2} + \frac{1}{(\kappa_0 + \pi_0 - i)^2} \right] \\ & = \frac{16}{9} \pi^2 \frac{1}{(\vec{k} + \vec{p})^2} \end{aligned} \quad (4.11)$$

which might be calculated with the contour method and does not vanish in contrast to the naive expectation that temporal modes should not contribute in calculations carried out in the temporal gauge. Whether temporal gauge modes and/or ghost fields yield non-vanishing contributions to observable quantities strongly depends on the pole prescription one uses for the  $k_0$ -pole in the longitudinal part of the gauge propagator.

This shows that infrared singularities in the propagator must be handled with extreme care. In principle the same holds true for UV-singularities caused by propagators which do not vanish at infinity. A prominent example is the temporal mode of the Coulomb propagator [9]

$$D^{00}(k) = \frac{i}{\vec{k}^2} \rightarrow \text{finite} \quad \text{for } k_0 \rightarrow \infty. \quad (4.12)$$

In the case at hand we should worry about infrared problems since they appear in the naive perturbation theory at finite temperature and cause the necessity of resummation. Indeed in our decomposition (c.f. (3.13))

$$-igf^{abc} \left( g_{\mu\nu} - \frac{k_\mu k_\nu}{k^2} \right) D_{\text{resum}}^{\nu\rho,cd}(k) = -igf^{abd} \frac{1}{k^2} g_{\mu\nu} + igf^{abd} \delta_{\mu 0} \delta_{\nu 0} \delta_{k_0 0} \frac{m^2}{k^2 (m^2 + k^2)} - G_\mu^{abd}(k) \frac{k_\nu}{k^2} \quad (4.13)$$

the terms at the r.h.s. have IR singularities. As we have shown in the previous sections the three terms are treated differently in further diagrammatic manipulations, e.g. the necessary momentum shifts for the first term of the r.h.s. of (4.13) is different from the ones for the third term. Thus loop integrals over the sum on the r.h.s. of (4.13) which are well-defined since the sum is IR safe have to be split in sums over loop integrals which might cause trouble. Fortunately these considerations are purely academic since the transverse projector  $\left(g_{\mu\nu} - \frac{k_\mu k_\nu}{k^2}\right)$  in (4.13) is *always* accompanied by a factor  $k^2$  which makes all terms at the r.h.s. of (4.13) IR safe (c.f. (3.13)). Thus in our calculations performed in the previous sections no IR singular terms ever appear. Of course this holds only true for covariant  $\alpha$ -gauges. Once axial gauges or the Coulomb gauge are used the considerations of this section might become relevant again.

Now we turn to the three loop diagrams and prove the gauge invariance (more precisely the  $\alpha$ -independence) of the QCD partition function as calculated up to  $\mathcal{O}(g^4)$  using the resummation scheme outlined in subsection III A.

## V. GAUGE INVARIANCE OF $Z_{\text{QCD}}$ AT $\mathcal{O}(g^4)$

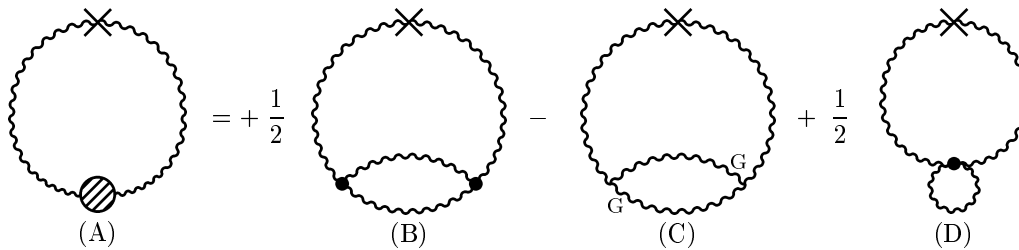
In this Section we prove the gauge invariance, more precisely the  $\alpha$ -independence of the  $\mathcal{O}(g^4)$  contributions to the partition function. Decomposing the corresponding diagrams of (3.18) with the help of the extended Cheng-Tsai rule (3.14), we obtain two different sets of diagrams:

- I. diagrams with the same graphical representation as the vacuum contributions but which have an implicit mass dependence stemming solely from the massive static gluon propagator  $D'_F$  in (3.10).
- II. diagrams which contain explicit mass terms, i.e., they contain “crosses” or “cross-stars”. These again split into two sets:
  - (a) diagrams in which the crosses arise from the mass counterterms (3.12/3.19) to the three-loop diagrams.
  - (b) diagrams in which the crosses arise from the additional terms in the identity (3.18) compared to (2.10), where an arrow pointing to a three-gluon vertex is decomposed.

To check the gauge-invariance of the set of diagrams I, one follows closely that of the vacuum case. It is a straightforward application of the original Cheng-Tsai rules discussed in Sec. II. The most important technical steps are given in Appendix A. This leaves us with the gauge-invariance check of the set II. Here, we analyse in a first Subsection the structure of IIa and we find that the  $\alpha$ -dependence of this set is given by the diagrams (5.2.E-G) below. In a second subsection, we turn then to the set IIb showing that its  $\mathcal{O}(g^4)$  contribution cancels exactly the remaining terms of IIa.

### A. Mass Counterterms to Three-Loop

We discuss now the two-loop diagrams of the perturbative expansion (3.18) of  $Z_{\text{QCD}}$  which occur as counterterms to the three-loop contribution:



$$\begin{array}{c}
- \text{ (E) } + \text{ (F) } \\
\text{ (5.1) }
\end{array}$$

Diagrams (5.1.C,E,F) contain the  $\alpha$ -independent, static gluon propagator only. The  $\alpha$ -independent part of the remaining two diagrams can be analysed with the help of (2.14) following the procedure of Sec. II C. Decomposing the  $\alpha$ -dependent parts of diagram (5.1.B), we obtain:

$$\begin{array}{c}
\text{ (A) } = - \text{ (B) } + * \text{ (C) } + \text{ (D) } \\
+ \text{ (E) } - \text{ (F) } \\
= + \text{ (B) } - \text{ (C) } - \text{ (D) } \\
+ * \text{ (E) } - \text{ (F) } + \text{ (G) } \\
\text{ (5.2) }
\end{array}$$

This allows for the following cancellations:

- (i) Diagram (5.2.B) cancels the  $\alpha$ -dependent part of (5.1.D). This is a consequence of the identity (2.17), relating a four-gluon vertex to two contracted three gluon vertices.
- (ii) The diagrams (5.2.C) and (5.2.D) cancel the  $\alpha$ -dependent  $\mathcal{O}(g^4)$  contributions (3.20) of the two-loop part (3.18.C-F) of  $Z_{\text{QCD}}$ . That both sets of diagrams have exactly the same structure follows from the identity (3.15) which relates a contraction arrow on a cross to a cross-star. It remains to show that the prefactors of (5.2.C),

(5.2.D) and (3.20) allow for cancellation.

To determine these prefactors, we first specify the symmetry factors attached to each diagram. Then, we symmetrize all diagrams according to the arguments of Sec. IID. For the three-loop contributions discussed here, this amounts to six gluon propagators to be symmetrized. Let us start with diagram (3.20). Their combinatorial factor is  $\frac{1}{12}$  and they represent an  $\alpha$ -dependent part of the basic diagram (2.21.B). Symmetrizing the latter with respect to its six different gluon propagators gives another factor  $\frac{1}{20}$ . The total prefactor of (3.20) is  $4 \cdot \frac{1}{12} \cdot \frac{1}{20} = \frac{1}{60}$ , since always four differently symmetrized versions of (2.21.B) lead to the same version of (3.20) upon decomposition, e.g.,

$$\begin{array}{ccc}
 D_3/D_4/D_5/D_6 & & \\
 \begin{array}{c} \text{Diagram (A): A circle with a horizontal wavy line labeled } D_2 \text{ in the middle. The top arc is labeled } D_3/D_4/D_5/D_6. \end{array} & \rightarrow & \begin{array}{c} \text{Diagram (B): A circle with a horizontal wavy line labeled } D_2 \text{ in the middle. The top arc has a cross with an asterisk.} \end{array} \\
 \text{(A)} & & \text{(B)}
 \end{array} \tag{5.3}$$

On the other hand, diagram (5.1.B) whose decomposition leads to (5.2.C) and (5.2.D), carries a combinatorial factor  $\frac{1}{4}$ . Symmetrization with respect to the possible gluon propagators gives a factor  $\frac{1}{15}$ . Consequently, the terms (5.2.C) and (5.2.D) have a total prefactor  $\frac{1}{60}$ , too, and cancel the contribution from (3.20). We are left with the diagrams (5.2.E-G) which must be treated together with the set of diagrams IIb.

### B. Three-Loop Diagrams with Explicit Mass Dependence

The complete set IIb of  $\alpha$ -dependent three-loop contributions which have an explicit mass dependence is given in the following eqs. (5.4) and (5.5):

$$\begin{array}{cccc}
 - & \begin{array}{c} \text{Diagram (A): Circle with } \Delta \text{ in the center, three wavy lines to the boundary. One line has a cross with an asterisk.} \end{array} & - & \begin{array}{c} \text{Diagram (B): Circle with } \Delta \text{ in the center, three wavy lines to the boundary. One line has a cross with an asterisk.} \end{array} \\
 & \text{(A)} & & \text{(B)} \\
 + & \begin{array}{c} \text{Diagram (C): Circle with } \Delta \text{ in the center, three wavy lines to the boundary. One line has a cross with an asterisk.} \end{array} & + & \begin{array}{c} \text{Diagram (D): Circle with } \Delta \text{ in the center, three wavy lines to the boundary. One line has a cross with an asterisk.} \end{array} \\
 & \text{(C)} & & \text{(D)} \\
 + & \begin{array}{c} \text{Diagram (E): Circle with } \Delta \text{ in the center, three wavy lines to the boundary. One line has a cross with an asterisk.} \end{array} & - & \begin{array}{c} \text{Diagram (F): Circle with } \Delta \text{ in the center, three wavy lines to the boundary. One line has a cross with an asterisk.} \end{array} \\
 & \text{(E)} & & \text{(F)} \\
 + & \begin{array}{c} \text{Diagram (G): Circle with } \Delta \text{ in the center, three wavy lines to the boundary. One line has a cross with an asterisk.} \end{array} & - & \begin{array}{c} \text{Diagram (H): Circle with } \Delta \text{ in the center, three wavy lines to the boundary. One line has a cross with an asterisk.} \end{array} \\
 & \text{(G)} & & \text{(H)} \\
 + & \begin{array}{c} \text{Diagram (I): Circle with } \Delta \text{ in the center, three wavy lines to the boundary. One line has a cross with an asterisk.} \end{array} & + & \begin{array}{c} \text{Diagram (J): Circle with } \Delta \text{ in the center, three wavy lines to the boundary. One line has a cross with an asterisk.} \end{array} \\
 & \text{(I)} & & \text{(J)} \\
 - & \begin{array}{c} \text{Diagram (K): Circle with } \Delta \text{ in the center, three wavy lines to the boundary. One line has a cross with an asterisk.} \end{array} & + & \begin{array}{c} \text{Diagram (L): Circle with } \Delta \text{ in the center, three wavy lines to the boundary. One line has a cross with an asterisk.} \end{array} \\
 & \text{(K)} & & \text{(L)}
 \end{array}$$

$$\begin{aligned}
& - \text{(M)} - \frac{1}{2} \Delta \text{(N)} + \frac{1}{2} \Delta \text{(O)} - \frac{1}{2} \Delta \text{(P)} \\
& + \frac{1}{2} \Delta \text{(Q)} - \frac{1}{4} \text{(R)} + \frac{1}{4} \text{(S)} \tag{5.4}
\end{aligned}$$

All the diagrams in (5.4) are at least of  $\mathcal{O}(g^5)$  as can be seen by splitting each loop integral into hard  $\mathcal{O}(T)$  and soft  $\mathcal{O}(m)$  momenta.

In contrast, some contributions from the “self-energy”-diagram (3.18.N) are  $\mathcal{O}(g^4)$ . In the following equation, all diagrams containing such  $\mathcal{O}(g^4)$ -parts are labelled with letters. The remaining diagrams, being  $\mathcal{O}(g^5)$  and higher are left unlabelled

$$\begin{aligned}
& - \frac{1}{2} \text{(A)} + \frac{1}{2} \text{(B)} + \frac{1}{2} \text{(C)} + \text{(unlabelled)} \\
& + \text{(unlabelled)} - \text{(unlabelled)} + \text{(unlabelled)} + \text{(unlabelled)} \\
& - \text{(unlabelled)} + \text{(unlabelled)} - \frac{1}{2} \text{(D)} - \frac{1}{2} \text{(E)}
\end{aligned}$$

$$\begin{aligned}
& + \frac{1}{2} \text{(F)} - \text{(G)} + \text{(H)} - \text{(I)} + \text{(J)} + \text{(K)} \\
& - \text{(L)} + \text{(M)} - \text{(N)} - \text{(O)} \\
& + \text{(P)} + \text{(Q)} - \text{(R)} - \frac{1}{2} \text{(S)} \\
& - \frac{1}{2} \text{(T)} + \frac{1}{2} \text{(U)} - \frac{1}{2} \text{(V)} + \frac{1}{2} \text{(W)} \\
& + \frac{1}{2} \text{(X)}
\end{aligned}
\tag{5.5}$$

The diagrams (F) through (X) are Feynman diagrams for a two-loop process. They consist of a main loop with two vertices (black dots) and two external lines (wavy lines). The vertices are labeled  $\Delta$  and the external lines are labeled  $G$ . The diagrams are characterized by the presence of a star ( $*$ ) and a cross ( $\times$ ) on the internal lines. The diagrams are arranged in a grid, with the first four rows containing four diagrams each, and the last row containing one diagram. The diagrams are labeled (F) through (X) in parentheses below them.

The  $\mathcal{O}(g^4)$ -parts of (5.5.A-X) are characterized by special contributions of hard (h) and soft (s) momenta in each

diagram. For these combinations one can cancel all  $\mathcal{O}(g^4)$ -parts with the help of two relations:

- (i) the definition of the Debye-mass (3.8/3.9) and
- (ii) the transversality of the one-loop self-energy.

Let us first focus on (i). As an example we show the  $\mathcal{O}(g^4)$ -parts of the diagrams (5.5.B/H/N/V) (note that the propagators with an explicit mass-dependence (the “cross-stars”) are always soft):

$$\frac{1}{2} \text{(A)} - \text{(B)} - \text{(C)} + \frac{1}{2} \text{(D)} \quad (5.6)$$

The definition of the one-loop Debye-mass (3.8/3.9) assures that the sum of the four diagrams above is just minus the diagram (5.2.E):

$$\text{(5.2.E)} \quad (5.7)$$

Consequently, these five diagrams cancel. In the same way we can identify the  $\mathcal{O}(g^4)$ -parts of the diagrams (5.5.A/G/M/W) with (5.2.F) and (5.5.C/I/O/X) with (5.2.G). Note that it is not surprising that the actual definition of the Debye mass enters at this stage of the calculation. If the mass  $m$  in the counterterm (3.12) is not defined properly via the static limit of the self energy, the result for the physical quantity of interest might be incorrect and gauge dependent.

Now we turn to argument (ii). We group the diagrams which are still left together to four-diagram blocks so that the sum can be depicted as one diagram which has a one-loop self-energy insertion. This insertion is always Lorentz-contracted with  $\Delta_\mu$ , which contains  $k_\mu$  for covariant gauges. Due to the known relation for the one-loop self-energy,

$$k_\mu \Pi^{\mu\nu} = 0, \quad (5.8)$$

these blocks of four diagrams are zero. To give an example, we look at the diagrams (5.5.D/J/P/S):

$$-\frac{1}{2} \text{(A)} + \text{(B)} + \text{(C)} - \frac{1}{2} \text{(D)} = - \text{(E)} \quad (5.9)$$

The same holds true for (5.5.E/K/Q/T) and (5.5.F/L/R/S). In this way  $\mathcal{O}(g^4)$ -contributions of gauge dependent parts of the three loop diagrams are cancelled. Thus we have proven that the partition function up to  $\mathcal{O}(g^4)$  is  $\alpha$ -independent for an arbitrary covariant gauge. Of course it would be interesting to extend the proof to  $\mathcal{O}(g^5)$ . Here, however, all diagrams of (5.4) and (5.5) contribute and so far we haven't found a way to prove their cancellation diagrammatically.

We briefly summarize the necessary steps to prove the  $\alpha$ -independence of a sum of loop diagrams in a general covariant gauge:

- Start with the diagram which has only three-gluon vertices (like (3.18.C) for the two-loop and (3.18.F) for the three-loop case). Decompose one gluon propagator according to (3.10). Then treat the rest of the diagrams in the same way.
- Use (3.14) and the equivalent of (2.12) as long as there are  $k_\mu$ -arrows pointing at a three-gluon vertex, (2.16) as long as there are such arrows pointing at a fermion-gluon vertex.
- Use (2.14) to pull arrows out of closed ghost loops (c.f. the last equality in (2.25)).
- At this stage all  $a_\mu$ -dependent diagrams which have neither contraction arrows nor four-point vertices should drop out.
- Next, diagrams with different topology are related by the rules of Sec. II. To get an idea which diagrams are related it is instructive to contract the lines with contraction arrows.
- In all remaining diagrams the momentum integrations have to be split up in hard and soft modes to figure out which diagrams contribute to the order of  $g$  one is interested in. The current definition of the Debye mass and the transversality of the one-loop self-energy has to be taken into account.
- All diagrams which have no counterparts so far ought to be of higher order in the coupling constant.
- Finally symmetry factors have to be counted as outlined in Secs. II D and V A.

In this article we have presented a method to check whether a resummation scheme preserves gauge invariance. This method is diagrammatic and relates systematically diagrams with different topology. This avoids tedious analytical calculations since it can be seen already at the diagrammatic level which algebraic expressions cancel each other. (This means that in a calculation the integrands cancel before performing the integrations.) Of course this diagrammatic method is less elegant than formal proofs of gauge invariance using Ward identities. On the other hand formal proofs are sometimes not straightforward or ambiguous due to singularities. Originally this diagrammatic method was invented by Cheng and Tsai [4] to check the consistency of different sets of Feynman rules for vacuum QCD. Here we have given an example that this method can be extended to check gauge invariance of physical quantities calculated in improved perturbation schemes. We have applied the diagrammatic method to the calculation of the free energy of finite temperature QCD up to  $O(g^4)$ .

Strictly speaking we have only shown that the result for the partition function/free energy is independent of  $\alpha$  for arbitrary covariant  $\alpha$ -gauges. In principle it should also be checked that the result remains the same if one performs the calculation in a different class of gauges like e.g. axial or Coulomb gauge. Thus from a rigorous point of view further investigations are required to prove the gauge invariance of  $Z_{\text{QCD}}$ . Of course the diagrammatic method outlined here is not restricted to covariant gauges but can be used for arbitrary gauges [4,20]. Note that then one has to deal with the momentum shift problems discussed in Sec. IV. In practice however  $\alpha$ -independence is often used synonymously for gauge invariance. Indeed e.g. the famous “plasmon puzzle” [1], i.e., the fact that the plasmon damping rate calculated without resummation turns out to be gauge dependent, already shows up for different values of  $\alpha$ .

We expect that the method presented here can be extended to more complicated resummation schemes (like e.g. “hard thermal loops” [2] where also vertex resummation is taken into account) and to electro-weak gauge theory (where the partition function in the vicinity of the phase transition is of special interest [21]). For the latter case we also refer to [22] where a similar diagrammatic method is used to minimize the computational effort for calculating S-matrix elements in vacuum quantum field theory.

## ACKNOWLEDGMENTS

We acknowledge enlightening discussions with Anton Rebhan and useful remarks by Markus Thoma. U.H. and S.L. would like to thank Prof. B. Müller and the Duke University Physics Department, where part of this work was done, for their kind hospitality. U.H. would like to thank CERN for warm hospitality and a stimulating atmosphere during the final stages of this work, too. This work was supported in part by BMBF, DFG and GSI.

In this Appendix, we give further details of how to prove the gauge invariance of the “vacuum like” three loop contributions to the QCD partition function.

The explicit mass dependent diagrams are discussed in Sec.V. In addition, the straightforward application of the diagrammatic rules of Sec. II to (3.18) results in approximately 100  $a_\mu$ -dependent diagrams. We have checked that the sum of these contributions cancels. For lack of space, we restrict our presentation here to a special example: The cancellation of all  $a_\mu$ -dependent contributions to star diagrams.

### Cancellation of the Star

Instead of presenting all diagrams we demonstrate for the star diagrams how the Cheng-Tsai rules work for three-loop diagrams. Then we outline briefly how all the other diagrams drop out.

1. The star diagrams allow the following decompositions:

$$(A) = (B) + 2 (C) \quad (A1)$$

$$- (A) = - (B) - (C) - (D) \quad (A2)$$

$$- (A) = - (B) - 2 (C) \quad (A3)$$

$$(A) = (B) + (C) + (D) \quad (A4)$$

$$\begin{array}{c} \text{(A)} \end{array} = \begin{array}{c} \text{(B)} \end{array} + 2 \begin{array}{c} \text{(C)} \end{array} \quad (\text{A5})$$

Note that to emphasize the structure of the decomposition (2.1), Cheng and Tsai have introduced slightly different notations for the two  $\Delta$ -dependent terms, one coming with  $\Delta(-k)$  and an overall  $+$  sign, the other with  $\Delta(k)$  and an overall  $-$  sign. To ease a purely diagrammatic analysis, we depart here from this notational convention. we use  $\Delta(k) = -\Delta(-k)$  such that all  $\Delta$  in the diagrams (A1) to (A5) are understood to represent factors  $\Delta(-k)$ . As a consequence, if the propagator (2.1) connects two vertices of the same type, then the orientation of the arrow does not matter, the two  $\Delta$ -dependent contributions are equal and can be summed up. This leads to the factors 2 in front of (A1.C), (A3.C) and (A5.C), while in (A2) and (A4) respectively, the arrows point on vertices of different types and both  $\Delta$ -dependent terms have to be dealt with separately.

- Using the rules from section II A, we can decompose each diagram further. Strictly speaking we should use (3.14) instead of (2.10). The additional contributions, however, show an explicit  $m$ -dependence. They are discussed separately in Sec. V. We begin with diagram (A1.C):

$$\begin{array}{c} \text{(A)} \end{array} \rightarrow 2 \left[ \begin{array}{c} \text{(B)} + \text{(C)} - \text{(D)} \\ - \text{(E)} - \text{(F)} + \text{(G)} \\ - \text{(H)} - \text{(I)} + \text{(J)} \end{array} \right]$$

$$\begin{aligned}
& + \text{(K)} - \text{(L)} + \text{(M)} \\
& - \text{(N)} + \text{(O)} + \text{(P)} \\
& - \text{(Q)} - \text{(R)} \quad \Bigg] \quad (1.6)
\end{aligned}$$

In the same way we treat the star diagrams containing ghosts. Diagram (A2.D) can be decomposed as follows:

$$\begin{aligned}
& - \text{(A)} \rightarrow - \text{(B)} - \text{(C)} \\
& + \text{(D)} + \text{(E)} \quad (1.7)
\end{aligned}$$

Some diagrams already cancel on this level of the calculation. To be specific:

(1.6.J) cancels (A3.C), (1.6.H) cancels (1.7.E), (1.6.P) cancels (1.7.C), (1.6.Q) cancels (A2.C).

The decomposition and cancellation of the star diagrams containing fermions will be discussed below.

3. The remaining star diagrams do not cancel each other but are related to diagrams with different topology. To make their cancellation clear we use the identities from section IIB, specially (2.17), (2.18) and (2.19).

We start with relation (2.17) and place the  $\Delta$  at the upper line near the left vertex. We connect the upper two lines with a three-gluon-vertex, we do the same with the lower ones, and we connect the remaining free leg of each vertex. In this way we get:

$$+ 2 \begin{array}{c} \text{Diagram (A)} \\ \text{A circular diagram with three wavy lines meeting at a central vertex. A triangle labeled } \Delta \text{ is formed by the upper two lines.} \end{array} - \begin{array}{c} \text{Diagram (B)} \\ \text{A circular diagram with three wavy lines meeting at a central vertex. A triangle labeled } \Delta \text{ is formed by the upper two lines, with an arrow pointing right.} \end{array} = - \begin{array}{c} \text{Diagram (C)} \\ \text{A circular diagram with three wavy lines meeting at a central vertex. A triangle labeled } \Delta \text{ is formed by the upper two lines, with an arrow pointing left.} \end{array} . \quad (1.8)$$

With this relation diagram (1.6.B) cancels  $\alpha$ -dependent parts from the diagrams (3.18.M) and (3.18.N) respectively. Now closing (2.17) in different ways and using a ghost-gluon vertex as well as a three-gluon vertex, one can find 12 more relations. With the help of these relations the diagrams (1.6.C), (1.6.D), (1.6.E), (1.6.L) are also cancelled by other diagrams.

For the star diagram, we need no identity derived from (2.18). However it is necessary to cancel diagrams originating from (3.18.M) and (3.18.N).

Finally we use (2.19). In an analogous way as above we get e.g. the following relation:

$$\begin{array}{c} \text{Diagram (A)} \\ \text{A circular diagram with three wavy lines meeting at a central vertex. A triangle labeled } \Delta \text{ is formed by the upper two lines.} \end{array} - \begin{array}{c} \text{Diagram (B)} \\ \text{A circular diagram with three wavy lines meeting at a central vertex. A triangle labeled } \Delta \text{ is formed by the upper two lines, with an arrow pointing right.} \end{array} - \begin{array}{c} \text{Diagram (C)} \\ \text{A circular diagram with three wavy lines meeting at a central vertex. A triangle labeled } \Delta \text{ is formed by the upper two lines, with an arrow pointing left.} \end{array} = 0. \quad (1.9)$$

At all one gets five relations out of (2.19) which cause the diagrams (1.6.F), (1.6.G), (1.6.I), (1.6.K), (1.6.M), (1.6.N), (1.6.O), (1.6.R), (1.7.B), (1.7.D) to cancel each other.

#### 4. Now we discuss the decomposition and cancellation of the star diagrams with fermions.

We only give a brief example of the cancellations. Decomposing e.g. (A4.C) in the way described above we get:

$$\begin{array}{c} \text{Diagram (A)} \\ \text{A circular diagram with three wavy lines meeting at a central vertex. A triangle labeled } \Delta \text{ is formed by the upper two lines.} \end{array} = \begin{array}{c} \text{Diagram (B)} \\ \text{A circular diagram with three wavy lines meeting at a central vertex. A triangle labeled } \Delta \text{ is formed by the upper two lines, with an arrow pointing right.} \end{array} - \begin{array}{c} \text{Diagram (C)} \\ \text{A circular diagram with three wavy lines meeting at a central vertex. A triangle labeled } \Delta \text{ is formed by the upper two lines, with an arrow pointing left.} \end{array} . \quad (1.10)$$

On the other hand we close the fermion identity (2.20) to find

$$- \begin{array}{c} \text{Diagram (A)} \\ \text{A circular diagram with three wavy lines meeting at a central vertex. A triangle labeled } \Delta \text{ is formed by the upper two lines.} \end{array} = + \begin{array}{c} \text{Diagram (B)} \\ \text{A circular diagram with three wavy lines meeting at a central vertex. A triangle labeled } \Delta \text{ is formed by the upper two lines, with an arrow pointing right.} \end{array} - \begin{array}{c} \text{Diagram (C)} \\ \text{A circular diagram with three wavy lines meeting at a central vertex. A triangle labeled } \Delta \text{ is formed by the upper two lines, with an arrow pointing left.} \end{array} . \quad (1.11)$$

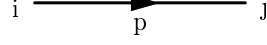
Hence the diagram (1.10.A) is cancelled by a diagram originating from (3.18.N). Similarly all  $a_\mu$ -dependent diagrams containing fermions cancel.

In the same way all  $a_\mu$ -dependent diagrams of (3.18) drop out of the calculation of the partition function.

## APPENDIX B: FEYNMAN RULES

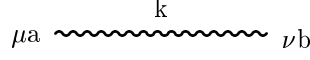
We use the following Feynman rules for covariant  $\alpha$ -gauges in Euklidien space-time:

fermion propagator



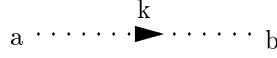
$$S_{ij} = -\frac{\delta_{ij}}{\not{p} - m_f}$$

gluon propagator



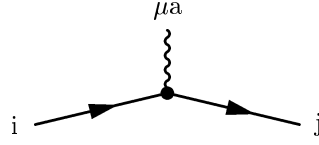
$$D_{\mu\nu}^{ab} = \frac{\delta^{ab}}{k^2} \left[ g_{\mu\nu} - (1 - \alpha) \frac{k_\mu k_\nu}{k^2} \right]$$

ghost propagator



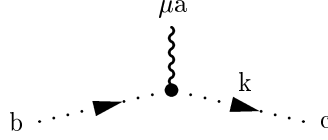
$$W^{ab} = -\frac{\delta^{ab}}{k^2}$$

fermion-gluon vertex



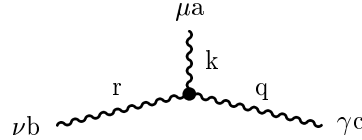
$$F_{\mu,ij}^a = -g\gamma_\mu t_{ij}^a$$

ghost-gluon vertex



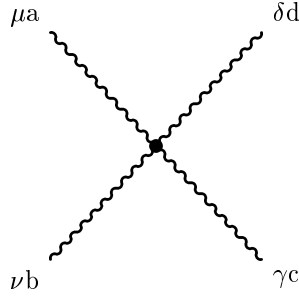
$$\Gamma_\mu^{abc} = -igf^{abc}k_\mu$$

three-gluon vertex



$$\Gamma_{\mu\nu\gamma}^{abc}(k, r, q) = -igf^{abc} [g_{\nu\gamma}(r - q)_\mu + g_{\mu\nu}(k - r)_\gamma + g_{\gamma\mu}(q - k)_\nu]$$

four-gluon vertex



$$Q_{\mu\nu\gamma\delta}^{abcd} = -g^2 [f^{ade}f^{ebc}(g_{\mu\nu}g_{\delta\gamma} - g_{\mu\gamma}g_{\delta\nu}) + f^{abe}f^{edc}(g_{\mu\delta}g_{\nu\gamma} - g_{\mu\gamma}g_{\delta\nu}) + f^{ace}f^{edb}(g_{\mu\delta}g_{\gamma\nu} - g_{\mu\nu}g_{\delta\gamma})]$$



\* On sabbatical leave from Institut für Theoretische Physik, Universität Regensburg, D-93040 Regensburg, Germany.

- [1] E. Braaten and R.D. Pisarski, Phys. Rev. **D42** (1990) 2156.
- [2] E. Braaten and R.D. Pisarski, Nucl. Phys. **B337** (1990) 569; **B339** (1990) 310.
- [3] R. Kobes, G. Kunstatter, and A. Rebhan, Phys. Rev. Lett. **64** (1990) 2992; Nucl. Phys. **B355** (1991) 1.
- [4] H. Cheng and E.-C. Tsai, MIT-preprint “The Theorem of Equivalence and The Anomalous Coulomb Interaction” (1986).
- [5] Y.J. Feng and C.S. Lam, Phys. Rev. **D53** (1996) 2115.
- [6] P. Arnold and C. Zhai, Phys. Rev. **D50** (1994) 7603.
- [7] P. Arnold and C. Zhai, Phys. Rev. **D51** (1995) 1906.
- [8] C. Zhai and B. Kastening, Phys. Rev. **D52** (1995) 7232.
- [9] H. Cheng and E.-C. Tsai, Phys. Rev. Lett. **57** (1986) 511.
- [10] H. Cheng and E.-C. Tsai, Chin. J. Phys. **25** (1987) 95.
- [11] P. Arnold and O. Espinosa, Phys. Rev. **D47** (1993) 3546.
- [12] E. Braaten and A. Nieto, Phys. Rev. **D51** (1995) 6990; Phys. Rev. **D53** (1996) 3421.
- [13] N.P. Landsman and Ch.G. van Weert, Phys. Rep. **C145** (1987) 141.
- [14] J. Kapusta, Nucl. Phys. **B148** (1979) 461.
- [15] A. Linde, Rep. Prog. Phys. **42** (1979) 389; Phys. Lett. **B96** (1980) 289.
- [16] J. Kapusta, Finite-Temperature Field Theory, Cambridge University Press, Cambridge, England (1989).
- [17] F. Karsch, M. Lütgemeier, A. Patkos, and J. Rank, hep-lat/9605031.
- [18] M. Achhammer, M. Thoma, and U.A. Wiedemann, in preparation.
- [19] S. Caracciolo, G. Curci, and P. Menotti, Phys. Lett. **B113** (1982) 311.
- [20] S. Leupold, TPR-96-19, Universität Regensburg preprint, submitted to Phys. Rev. D
- [21] W. Buchmüller, Z. Fodor, and A. Hebecker, Nucl. Phys. **B447** (1995) 317.
- [22] Y.J. Feng and C.S. Lam, hep-ph/9608219.